

Synchronization of two bacterial flagella as a stochastic process

Jing Qin and Nariya Uchida*

Department of Physics, Tohoku University, Sendai 980-8578, Japan

(Dated: November 28, 2024)

Synchronization with noise is important for understanding biophysical processes at nano- and micro-meter scales, such as neuron firing and beating of cilia. To understand the energetics of these processes, stochastic thermodynamics approaches are useful. Due to large fluctuations in a small system, ensemble averages of thermodynamic quantities are not sufficient to characterize the energetics of an individual sample. In this paper, we use a model for synchronization of bacterial flagella as an example, and develop an approximation method for analyzing the phase and heat dissipation in trajectories for different noise realizations. We describe the time development of the phase difference and heat dissipation as stochastic processes, and verify the analytical results by numerical simulations.

Introduction.— Synchronization is ubiquitously seen in Nature. Since Huygens' discovery of synchronization in two pendulum clocks [1, 2], the study of synchronization has expanded across various fields [3]. In biological systems, synchronization plays a critical role in maintaining normal functions, such as regulating circadian rhythms [4], coordinating brain activity [5], and enabling flagellar movement [6–8]. This essential phenomenon has sparked extensive research, with the Kuramoto model [9, 10] emerging as a widely-used framework based on phase oscillators. In this study, we explore a related but distinct model employing a similar phase approach.

Flagella provide a classic example of synchronization driven by hydrodynamic interactions, generating considerable interest in the field. Powered by molecular motors, flagella create rhythmic fluid movements that propel microorganisms forward, forming metachronal waves [11, 12]. While some studies indicate that other factors may contribute to flagellar synchronization [13, 14], hydrodynamic interactions alone are often sufficient for modeling this behavior [15]. Due to the cyclic motion of flagella, they are frequently represented with simplified cyclic models [16, 17]. Additionally, as flagella operate at microscopic scales, thermal fluctuations from the surrounding environment significantly influence their movement, making it essential to consider stochastic effects alongside deterministic dynamics [18, 19].

Numerous studies have examined synchronization under the influence of noise [14, 20–23]. For instance, in [21], the authors explore a noise-driven model of two oscillators, showing that synchronization minimizes energy associated with the coupling's odd component, though specific hydrodynamic models may instead maximize energy. The energy dynamics involved in synchronization are critical for understanding energetic efficiency in living systems [24]. However, many studies focus on noise-averaged dynamics, which may overlook significant fluctuations.

In this research, we examine a specific model of two synchronized flagella with cyclic trajectories influenced

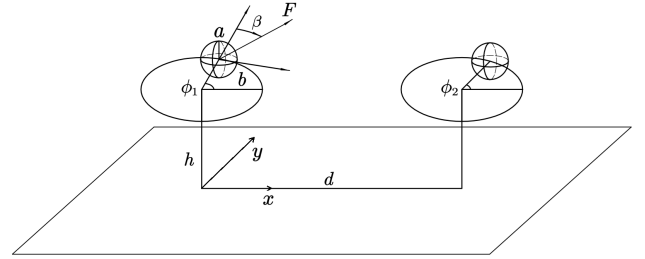


FIG. 1. Schematic picture of two flagella. Each sphere rotates on the circular trajectory of radius b , exerting the force F , which is tilted from the radial direction by the angle β in the clockwise direction, on the surrounding fluid.

by white noise. This model allows us to analytically investigate not only the statistical properties but also the single-trajectory dynamics without averaging. We validate our theoretical findings through numerical simulations.

Model.— Following Ref. [7], we consider flagella tethered to a substrate as active rotors that move by pumping the fluid. We take the xy -coordinates on the substrate and assume that a pair of rotors are fixed on it with distance d along the x -axis, as shown in Fig. 1. Each rotor has a spherical bead of radius a , which is connected to the substrate by an L-shaped filament. The filament consists of a vertical shaft of height h , which is the rotation axis of the rotor, and a horizontal arm with length b , which gives the radius of the circular trajectory of the bead. Using the polar angle ϕ_i of the i -th rotor, the positions of the two beads are represented by $\mathbf{r}_1 = h\mathbf{e}_z + b\mathbf{n}_1$ and $\mathbf{r}_2 = d\mathbf{e}_x + h\mathbf{e}_z + b\mathbf{n}_2$, where \mathbf{e}_i ($i = x, z$) is the unit vector along the x - and z -axis, respectively, and $\mathbf{n}_i(t) = (\cos\phi_i(t), \sin\phi_i(t), 0)$ gives the direction of the rotor's arm. The velocity of the bead reads $\mathbf{v}_i = \frac{d}{dt}\mathbf{r}_i = b\frac{d}{dt}\mathbf{n}_i = b\frac{d\phi_i}{dt}\mathbf{t}_i$, where $\mathbf{t}_i = (-\sin\phi_i, \cos\phi_i, 0)$ is the unit tangential vector of the orbit. A tethered flagellum pumps the surrounding fluid by the activity of the flagellar motor, which is modeled by a constant force exerted by the bead on the fluid. We decom-

pose the force \mathbf{F}_i exerted by the i -th bead ($i = 1, 2$) as $\mathbf{F}_i = F_r \mathbf{n}_i + F_\phi \mathbf{t}_i + F_z \mathbf{e}_z$, where F_r, F_ϕ, F_z are constants. In a low Reynolds number condition, the forces generate the flow velocity field $\mathbf{v}(\mathbf{r}) = \mathbf{G}(\mathbf{r} - \mathbf{r}_1) \cdot \mathbf{F}_1 + \mathbf{G}(\mathbf{r} - \mathbf{r}_2) \cdot \mathbf{F}_2$, where \mathbf{G} is the Green function of the Stokes equation. The Green function under the no-slip boundary condition on the substrate is known as the Blake tensor [25]. For $\mathbf{r} = \mathbf{r}_2 - \mathbf{r}_1 \simeq d \mathbf{e}_x$ with $d \gg h, b, a$, we obtain $\mathbf{G}(\mathbf{r}) \simeq 3h^2/(2\pi\eta d^3) \mathbf{e}_x \mathbf{e}_x$, where η is the shear viscosity.

In the overdamped limit, the motion of rotors is determined by the balance of three forces: the driving force, the resistance force and the thermal fluctuation force. The driving force is the reaction of the force exerted by the flagellum on the fluid and is given by $-F_\phi \mathbf{t}_i$ for the i -th rotor. The tangential component of the viscous resistance force is given by $F_{\text{viscous}} = \mathbf{t}_i \cdot \zeta (\frac{d}{dt} \mathbf{r}_i - \mathbf{v}(\mathbf{r}_i))$, where $\zeta = 6\pi\eta a$ is the resistance coefficient. The thermal fluctuation force is $F_{\text{thermal}} = \sqrt{2k_B T \zeta} \xi_i$, where ξ_i is a white Gaussian noise satisfying $\langle \xi_i(t) \xi_i(t') \rangle = \delta(t - t')$. It is defined as $\xi_i = dW_t^{(i)}/dt$ using the standard Wiener process $W_t^{(i)}$, and has the dimension of $t^{-\frac{1}{2}}$. The equation of force balance $-F_\phi + F_{\text{viscous}}^{(i)} + F_{\text{thermal}}^{(i)} = 0$ gives the Langevin equation,

$$\zeta b \frac{d\phi_i}{dt} = -F_\phi + \frac{9ah^2}{d^3} (F_\phi \sin \phi_2 - F_r \cos \phi_2) \sin \phi_1, \quad (1)$$

$$\zeta b \frac{d\phi_2}{dt} = -F_\phi + \frac{9ah^2}{d^3} (F_\phi \sin \phi_1 - F_r \cos \phi_1) \sin \phi_2 + \sqrt{2k_B T \zeta} \xi_2. \quad (2)$$

We assume $F_\phi < 0$ so that each rotor has a positive intrinsic phase velocity. Let $F = \sqrt{F_\phi^2 + F_r^2}$ and $\beta = \arctan(-F_\phi/F_r)$ ($0 \leq \beta \leq \pi/2$). As shown in Fig. 1, β represents the tilt of the force from the radial direction, which can be originated from the deviation of the flagellar axis from the anchoring point. For convenience, we introduce the two characteristic frequencies $\omega = F/(\zeta b)$ and $\omega_\phi = -F_\phi/(\zeta b)$ with the relation $\omega_\phi = \omega \sin \beta$. We also define the dimensionless quantities $K = 9ah^2/d^3$ and $D = k_B T/(Fb)$ to express the relative strengths of hydrodynamic and thermal forces, respectively. Then the equations of motion become

$$\frac{d\phi_1}{dt} = \omega_\phi - K\omega \cos(\phi_2 + \beta) \sin \phi_1 + \sqrt{2D\omega} \xi_1, \quad (3)$$

$$\frac{d\phi_2}{dt} = \omega_\phi - K\omega \cos(\phi_1 + \beta) \sin \phi_2 + \sqrt{2D\omega} \xi_2. \quad (4)$$

For typical flagella operating in water, we estimate the parameter values as $a \sim b \sim h \sim 1 \mu\text{m}$, $d \sim 10 \mu\text{m}$, $F \sim 10 \text{ pN}$, $k_B T \sim 4 \times 10^{-21} \text{ J}$ and $\eta \sim 10^{-3} \text{ Pa} \cdot \text{s}$. Thus we have $\omega \sim 10 \text{ Hz}$, $K \sim 10^{-2}$ and $D \sim 10^{-4}$. (Note that ω is not the flagellar rotation frequency, which is on

the order of $10^2 - 10^3 \text{ Hz}$ and is not considered in the present model.)

Steady state distribution.— To analyze the system's behavior in the steady state, we first consider the case $\sin \beta \gg K, \sqrt{D}$, where the intrinsic phase velocity dominates the hydrodynamic and thermal velocities (the second and third terms on the right-hand side of Eqs. (3),(4), and introduce the slow variable $\Phi_i = \phi_i - \omega_\phi t$. Using these, we rewrite Eqs. (3), (4) as

$$\frac{d\Phi_1}{dt} = \frac{K\omega}{2} A(\Phi_2, \Phi_1) + \sqrt{2D\omega} \xi_1, \quad (5)$$

$$\frac{d\Phi_2}{dt} = \frac{K\omega}{2} A(\Phi_1, \Phi_2) + \sqrt{2D\omega} \xi_2, \quad (6)$$

where

$$A(\Phi_i, \Phi_j) = \sin(\Phi_i - \Phi_j + \beta) - \sin(\Phi_i + \Phi_j + 2\omega t + \beta). \quad (7)$$

The corresponding Fokker-Planck equation for the probability distribution function $P(\Phi_1, \Phi_2; t)$ read:

$$\frac{\partial P}{\partial t} = -\frac{K\omega}{2} \left\{ \frac{\partial}{\partial \Phi_1} [A(\Phi_2, \Phi_1)P] + \frac{\partial}{\partial \Phi_2} [A(\Phi_1, \Phi_2)P] \right\} + D\omega \left(\frac{\partial^2}{\partial \Phi_1^2} + \frac{\partial^2}{\partial \Phi_2^2} \right) P. \quad (8)$$

We integrate the equation over the period π/ω under the slow-variable approximation that Φ_i 's remain unchanged, the second term of $A(\Phi_i, \Phi_j)$ vanish. For the stationary state where $\partial P/\partial t = 0$, we obtain

$$0 = -\frac{K}{2} \left\{ \frac{\partial}{\partial \Phi_1} [\sin(\Phi_2 - \Phi_1 + \beta)P] + \frac{\partial}{\partial \Phi_2} [\sin(\Phi_1 - \Phi_2 + \beta)P] \right\} + D \left(\frac{\partial^2}{\partial \Phi_1^2} + \frac{\partial^2}{\partial \Phi_2^2} \right) P. \quad (9)$$

Solving the above equation, we obtain the steady-state distribution

$$P(\Phi_1, \Phi_2) = \frac{1}{Z} \exp \left[\frac{K}{2D} \cos \beta \cos(\Phi_2 - \Phi_1) \right], \quad (10)$$

or equivalently

$$P(\phi_1, \phi_2) = \frac{1}{Z} \exp \left[\frac{K}{2D} \cos \beta \cos(\phi_2 - \phi_1) \right], \quad (11)$$

in terms of the original variables, where Z is the normalization factor given by

$$Z = 16\pi^2 I_0 \left(\frac{K}{2D} \cos \beta \right), \quad (12)$$

where $I_0(x)$ is the 0-th order modified Bessel function. The steady state distribution (11) is the von-Mises distribution for the phase difference. The flagella are more

likely be synchronized ($\phi_1 = \phi_2$) for a stonger coupling K and weaker noise D . Synchronization is also facilitated by a smaller force angle β ; for $\beta = \frac{\pi}{2}$, the distribution becomes flat and the system shows no tendency toward synchronization. For a strong coupling, the harmonic approximation $\cos(\phi_2 - \phi_1) \sim 1 - \frac{1}{2}(\phi_2 - \phi_1)^2$ gives a Gaussian distribution of the phase difference $\delta = \phi_2 - \phi_1$ with the standard deviation $\sqrt{2D/(K \cos \beta)}$. The stochastic entropy for a single state is defined by $s = -k_B \ln P$ [18]. Using the stationary distribution (11), we get

$$s(\phi_1, \phi_2) = k_B \left[\ln Z - \frac{K}{2D} \cos \beta \cos(\phi_2 - \phi_1) \right]. \quad (13)$$

The synchronized state minimizes the stochastic entropy reflecting its high order.

Heat dissipation.— In stochastic thermodynamics, for a particle satisfying the overdamped Langevin equation

$$\gamma \dot{x} = F(x, t) + \sqrt{2\gamma T} \xi, \quad (14)$$

the heat dissipation during an infinitesimal displacement dx is defined as [18, 26]

$$dQ = F \circ dx = (\gamma \dot{x} - \sqrt{2\gamma T} \xi) \circ dx, \quad (15)$$

where \circ denotes the Stratonovich product. Applying the definition, heat dissipation by the rotor 1 is written as

$$dQ_1 = \zeta b^2 [\omega_\phi - K\omega \cos(\phi_2 + \beta) \sin \phi_1] \circ d\phi_1. \quad (16)$$

For convenience, we consider heat without coefficient ζb^2 :

$$dQ'_1 = \frac{dQ_1}{\zeta b^2} = [\omega_\phi - K\omega \cos(\phi_2 + \beta) \sin \phi_1] \circ d\phi_1. \quad (17)$$

The heat dissipation by the rotor 2 is obtained similarly. The total heat dissipation in an arbitrary time period $0 < t < T$ under the initial condition $\phi_1(0) = \phi_2(0) = 0$ is obtained as, using partial integration,

$$\begin{aligned} Q' &= \int_0^T (dQ'_1 + dQ'_2) \\ &= \omega_\phi(\phi_1 + \phi_2) + K\omega [\cos(\phi_2 + \beta) \cos \phi_1 - \cos \beta] \\ &\quad + K\omega \int_0^{\phi_2} \sin \beta \cos(\phi_2 - \phi_1) \circ d\phi_2. \end{aligned} \quad (18)$$

Next we compute the heat specifically by solving the stochastic equations (3,4) for the phase $\phi_i(t)$. We change the variables to $\delta = \phi_1 - \phi_2$ and $\sigma = \phi_1 + \phi_2$ in Eqs.(3,4). For the phase difference, we obtain

$$\frac{d\delta}{dt} = -K\omega \cos \beta \sin \delta + 2\sqrt{D\omega} \xi_-, \quad (19)$$

where $\xi_- = (\xi_1 - \xi_2)/\sqrt{2}$. Assuming that the phase difference is small, we approximate $\sin \delta$ by δ and solve the equation as

$$\begin{aligned} \delta(t) &= 2\sqrt{D\omega} e^{-K\omega \cos \beta \cdot t} \int_0^t e^{K\omega \cos \beta \cdot s} dW_s \\ &= 2\sqrt{D\omega} \left(W_t - K\omega \cos \beta \int_0^t e^{K\omega \cos \beta \cdot (s-t)} W_s ds \right). \end{aligned} \quad (20)$$

Using this, we find $\langle \delta \rangle = \langle \phi_1 - \phi_2 \rangle = 0$ since the product is taken in Itô's sense. The variance reads

$$\begin{aligned} V(t) &= \langle (\delta(t))^2 \rangle \\ &= 4D\omega e^{-2K\omega \cos \beta \cdot t} \int_0^t e^{2K\omega \cos \beta \cdot s} ds \\ &= \frac{2D}{K \cos \beta} - \frac{2D}{K \cos \beta} e^{-2K\omega \cos \beta \cdot t}. \end{aligned} \quad (21)$$

In the long time limit, it converges to the equilibrium value $2D/(K \cos \beta)$ from below. From this, we confirm that the small phase difference approximation is satisfied either when $2D/(K \cos \beta) \ll 1$ or in a sufficiently short time.

$$\begin{aligned} \frac{d\sigma}{dt} &= 2\omega_\phi - K\omega \sin(\sigma + \beta) + K\omega_\phi \cos(\delta) \\ &\quad + 2\sqrt{D\omega} \xi_+. \end{aligned} \quad (22)$$

Using $\Phi_i = \phi_i - \omega_\phi t$ and $\Sigma = \Phi_1 + \Phi_2$ it can be rewritten as

$$\begin{aligned} \frac{d\Sigma}{dt} &= K\omega \sin(\Sigma + \beta + 2\omega_\phi t) - K\omega \cos \Delta \sin \beta \\ &\quad + 2\sqrt{D\omega} \xi_+. \end{aligned} \quad (23)$$

From this and Eq.(19), the change of Φ_i is proportional to the dimensionless parameters K and \sqrt{D} . that are in the slow variable approximation where $\sin \beta \gg K, \sqrt{D}$. We obtain Σ to the first order in K and \sqrt{D} as

$$\begin{aligned} \Sigma(t) &= K\omega_\phi t + \frac{K\omega}{2\omega_\phi} [\cos(2\omega_\phi t + \beta) - \cos \beta] \\ &\quad + 2\sqrt{D\omega} W_t \end{aligned} \quad (24)$$

Retaining only the terms in the first order of K and \sqrt{D} in Eq.(20), we obtain $\delta(t) = 2\sqrt{D\omega} W_t$. Combining this and Eq.(24), and using the definition $\Phi_i = \phi_i - \omega_\phi t$, we obtain

$$\begin{aligned} \phi_i(t) &= \omega_\phi \left(1 + \frac{K}{2} \right) t + \frac{K\omega}{4\omega_\phi} [\cos(2\omega_\phi t + \beta) - \cos \beta] \\ &\quad + \sqrt{2D\omega} W_t^{(i)} \end{aligned} \quad (25)$$

where W_i is Wiener process and the coefficient before that is also from the addition of two noise, and

$$\begin{aligned} Q'(t) &= 2\omega_\phi^2(1 + K)t - 2K\omega \sin(\omega_\phi t + \beta) \sin \omega_\phi t \\ &\quad + 2\omega_\phi \sqrt{D\omega} W_t \end{aligned} \quad (26)$$

The first term shows the linear time dependence, the second term is periodic with the period π/ω_ϕ , and the last term is a Brownian term with increment of \sqrt{t} .

Numerical analysis.— In the analytical treatment, we used two approximations: (i) slow variable, and (ii) small phase difference. The approximation (i) holds for $\sin \beta \gg K, \sqrt{D}$, while (ii) is valid if $\cos \beta \gg D/K$. We used (i) to obtain the distribution (11), and (ii) for time-evolution of the phase difference (20), and both of them for in time-evolution of phase(25) and heat dissipation (26). In order to verify these results and study the cases beyond the approximations, we performed numerical analysis by varying β as the control parameter. We integrated Eqs.(3),(4) for the phases $\phi_i(t)$ using the Euler-Maruyama method, and Eq.(15) for Q'_1 and a similar equation for Q'_2 with $\phi(t + \Delta t/2) \simeq (\phi_i(t + \Delta t) + \phi_i(t))/2$ for the Stratonovich product using the semi-implicit scheme. The time increment $\Delta t = 10^{-4}$ is used for both sets of equations. We took 10^3 independent samples for the noise for statistical analysis. Below we focus on three representative cases: $\beta = 0.01\pi, 0.25\pi$, and 0.49π .

For $\beta = 0.01\pi$, the approximation (i) is not valid, while (ii) holds. Comparing the first and third terms on the right hand side of Eq.(26), we expect a relatively large fluctuation effect for $t < \sqrt{D\omega}/\omega_\phi \sim 1$ s. We plot the mean $E_Q(t) = \langle Q'(t) \rangle$ and the standard deviation $\sigma'_Q(t) = \sqrt{\langle Q'(t)^2 \rangle - \langle Q'(t) \rangle^2}$ of the heat dissipation in Fig. 2(a) and the ratio $R = \sigma_Q/E_Q$ in Fig. 2(b). The ratio is large for short time, meeting our expectation. In Fig.2(a), $E_Q(t)$ shows a feature of the superposition of linear increase and periodic motion. The slope of that is almost the same as $2\omega_\phi^2 \approx 0.2$ in (26). The curves also show a periodic part with period $T = 10$ s, which comes from the term $\sin(\omega_\phi t + \beta) \sin \omega_\phi t$.

For $\beta = 0.25\pi$, where both the approximations (i),(ii) are valid, we consider time-evolution of the variance of the phase difference $V_\delta(t) = \langle (\delta)^2 \rangle = \langle (\phi_2 - \phi_1)^2 \rangle$ and the variance of the heat dissipation $V_Q(t) = \langle Q(t)^2 \rangle - \langle Q(t) \rangle^2$ in Fig.3. We choose the ending the time as 100s to see both initial and steady behavior. The results are in good agreement with our theoretical results; $V(\Delta\phi)$ increases exponentially with time as in Eq.(20), while $V(Q')$ linear increases with the slope $4\omega_\phi^2 D\omega = 0.2$ as in Eq.(26).

For $\beta = 0.49\pi$, the slow variable approximation holds but the small phase difference breaks down for a long time scale. We also draw the time development of the variance of heat dissipation in Fig. 3(b). From the figure, we find that in a small time, the variance increases linearly as shown by Eq.(26). However, in the long term, this turns to a power law increase with the exponent 3, which is not predicted by the theory.

Conclusion.— In this paper, we proposed an analytical method to compute the motion and heat dissipation of interacting flagella for individual noise realizations. We solved the phase difference and heat dissipation explicitly under the the slow variable and strong cou-

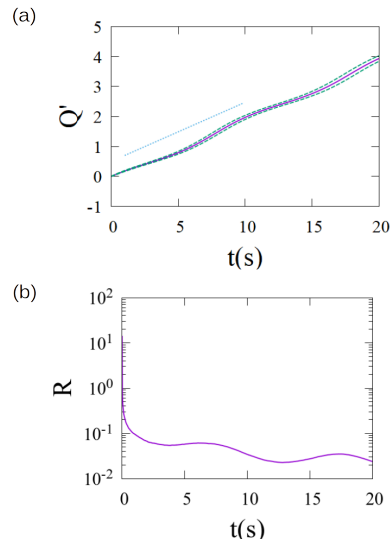


FIG. 2. The case $\beta = 0.01\pi$. (a) Dimensionless heat versus time. The solid line shows the ensemble average $\langle Q' \rangle$ and the dashed lines show $E(Q') = \langle Q' \rangle \pm \sigma(Q')$, where $\sigma(Q') = \sqrt{\langle Q'^2 \rangle - \langle Q' \rangle^2}$ is the standard deviation. The dotted line shows the slope $2\omega_\phi^2$. (b) The relative fluctuation $R = \sigma_Q/E_Q$ versus time (semi-log plot).

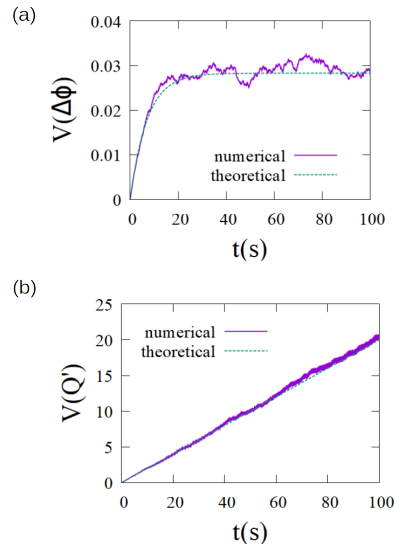


FIG. 3. Variation of (a) the phase difference $\Delta\phi$ and (b) the dimensionless heat Q' versus time for $\beta = 0.25\pi$. The solid lines show the numerical results, and the dotted lines show the theoretical results [Eqs.(20),(26)]

pling approximations. We compared the results with numerical simulations for three different parameter ranges. The results show a good correspondence where the two approximations are both valid. A possible future direction is to extend the analysis to many flagella, and analyze the heat dissipation in collective synchronization. Because the model is of a generic form, it can be applied to other mesoscale systems where thermody-

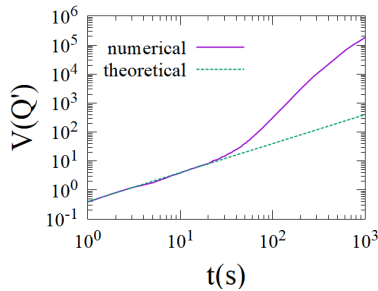


FIG. 4. Variation of the dimensionless heat for $\beta = 0.49\pi$. The solid line shows the numerical result and the dotted line shows the theoretical result.

dynamic noise affects but does not destroy synchronization.

Acknowledgment.— This work was supported by JSPS KAKENHI Grant Number JP24K06895 to N. U.

* uchida@cmpt.phys.tohoku.ac.jp

- [1] R. Dilão, *Chaos* **19**, 023118 (2009).
- [2] M. Kapitaniak, K. Czolczynski, P. Perlikowski, A. Stefanski, and T. Kapitaniak, *Phys. Rep.* **517**, 1 (2012).
- [3] S. Strogatz, *Sync: The emerging science of spontaneous order* (Penguin UK, 2004).
- [4] S. M. Reppert and D. R. Weaver, *Nature* **418**, 935 (2002).
- [5] O. Sporns, *Networks of the Brain* (MIT press, 2016).
- [6] A. Vilfan and F. Jülicher, *Phys. Rev. Lett.* **96**, 058102 (2006).
- [7] N. Uchida and R. Golestanian, *Phys. Rev. Lett.* **104**, 178103 (2010).
- [8] N. Uchida, R. Golestanian, and R. R. Bennett, *J. Phys. Soc. Jpn.* **86**, 101007 (2017).
- [9] J. A. Acebrón, L. L. Bonilla, C. J. Pérez Vicente, F. Ritort, and R. Spigler, *Rev. Mod. Phys.* **77**, 137 (2005).
- [10] Y. Kuramoto, *Chemical turbulence* (Springer, 1984).
- [11] S. Gueron and K. Levit-Gurevich, *Proc. Natl. Acad. Sci. (USA)* **96**, 12240 (1999).
- [12] B. Guirao and J.-F. Joanny, *Biophys. J.* **92**, 1900 (2007).
- [13] N. Naremsatsu, R. Quek, K.-H. Chiam, and Y. Iwadata, *Cytoskeleton* **72**, 633 (2015).
- [14] E. Hamilton, N. Pellicciotta, L. Feriani, and P. Cicuta, *Philos. Trans. R. Soc. B* **375**, 20190152 (2020).
- [15] J. Elgeti and G. Gompper, *Proc. Natl. Acad. Sci. (USA)* **110**, 4470 (2013).
- [16] J. Kotar, L. Debono, N. Bruot, S. Box, D. Phillips, S. Simpson, S. Hanna, and P. Cicuta, *Phys. Rev. Lett.* **111**, 228103 (2013).
- [17] R. E. Goldstein, M. Polin, and I. Tuval, *Phys. Rev. Lett.* **103**, 168103 (2009).
- [18] N. Shiraiishi, *An Introduction to Stochastic Thermodynamics* (Springer, 2023).
- [19] L. Peliti and S. Pigolotti, *Stochastic thermodynamics: an introduction* (Princeton University Press, 2021).
- [20] J.-n. Teramae and D. Tanaka, *Phys. Rev. Lett.* **93**, 204103 (2004).
- [21] Y. Izumida, H. Kori, and U. Seifert, *Phys. Rev. E* **94**, 052221 (2016).
- [22] A. Solovev and B. M. Friedrich, *Chaos* **32** (2022).
- [23] H. Hong, J. Jo, C. Hyeon, and H. Park, *J. Stat. Mech.* **2020**, 074001 (2020).
- [24] X. Yang, M. Heinemann, J. Howard, G. Huber, S. Iyer-Biswas, G. Le Treut, M. Lynch, K. L. Montooth, D. J. Needleman, S. Pigolotti, *et al.*, *Proc. Natl. Acad. Sci. (USA)* **118**, e2026786118 (2021).
- [25] J. R. Blake, *Math. Proc. Camb. Philos. Soc.* **70**, 303 (1971).
- [26] K. Sekimoto, *Stochastic Energetics*, Lecture Notes in Physics (Springer Berlin Heidelberg, 2010).